MEASURING SURFACE DYNAMICS OF BIOMOLECULES BY TOTAL INTERNAL REFLECTION FLUORESCENCE WITH PHOTOBLEACHING RECOVERY OR CORRELATION SPECTROSCOPY

NANCY L. THOMPSON, THOMAS P. BURGHARDT, AND DANIEL AXELROD,
Biophysics Research Division and Department of Physics, University of Michigan, Ann Arbor, Michigan 48109 U.S.A.

ABSTRACT The theoretical basis of a new technique for measuring equilibrium adsorption/desorption kinetics and surface diffusion of fluorescent-labeled solute molecules at solid surfaces has been developed. The technique combines total internal reflection fluorescence (TIR) with either fluorescence photobleaching recovery (FPR) or fluorescence correlation spectroscopy (FCS). A laser beam totally internally reflects at a solid/liquid interface; the shallow evanescent field in the liquid excites the fluorescence of surface adsorbed molecules. In TIR/FPR, adsorbed molecules are bleached by a flash of the focused laser beam; subsequent fluorescence recovery is monitored as bleached molecules exchange with unbleached ones from the solution or surrounding nonilluminated regions of the surface. In TIR/FCS, spontaneous fluorescence fluctuations due to individual molecules entering and leaving a well-defined portion of the evanescent field are autocorrelated. Under appropriate experimental conditions, the rate constants and surface diffusion coefficient can be readily obtained from the TIR/FPR and TIR/FCS curves. In general, the shape of the theoretical TIR/FPR and TIR/FCS curves depends in a complex manner upon the bulk and surface diffusion coefficients, the size of the illuminated or observed region, and the adsorption/desorption kinetic rate constants. The theory can be applied both to specific binding between immobilized receptors and soluble ligands, and to nonspecific adsorption processes. A discussion of experimental considerations and the application of this technique to the adsorption of serum proteins on quartz may be found in the accompanying paper (Burghardt and Axelrod. 1981. *Biophys. J.* 33:455).

INTRODUCTION

Biochemical reactions involving association of a molecule dissolved in solution with a target confined to a two-dimensional surface are of considerable industrial, medical, and biological importance. For example, biochemical products may be manufactured from substrate reactions with surface-immobilized enzymes which can be easily separated from the reaction and reused (1, 2). Surface immobilized antigens can be used to assay for the presence of specific antibodies in blood serum (3, 4). A wide variety of small soluble molecules interact with specific receptors on biological cell surfaces. It is possible that nonspecific adsorption of solute molecules followed by surface diffusion can dramatically enhance reaction rates with specific receptor sites on the surface (5). Data gathered on model biochemical systems (6, 7) indirectly suggest that such rate enhancement may indeed occur in living systems. We present here the theoretical basis of a technique for directly measuring the rate parameters critical to these processes; i.e., the adsorption and desorption rate constants and the surface diffusion

coefficient of solute molecules at a surface. Theoretical treatments concerning molecules in solution reacting with one- or two-dimensional structures have been previously presented (5, 8–13).

The technique has two variants which combine total internal reflection fluorescence (TIR) (12–17) with either fluorescence photobleaching recovery (FPR or FRAP) (18, 19) or fluorescence correlation spectroscopy (FCS) (16, 20–25). The experiments require no intrinsic spectroscopic difference between surface bound and unbound states of the solute molecules. In addition, no macroscopic departure from chemical equilibrium between bulk solubilized and surface adsorbed states is involved. The binding process may be either nonspecific (such as blood proteins adsorbed to a solid/liquid interface) or specific (such as soluble ligands binding to a surface bound receptor or soluble antibody binding to a surface bound antigen).

The physical bases of the two variants of the technique are similar. Fluorescent-labeled biomolecules are in chemical equilibrium between bulk solution and a solid surface to which they can adsorb. A laser beam totally internally reflects at the solid/liquid interface, creating an evanescent field which penetrates only a fraction of a wavelength into the liquid domain (reference 14, p. 30). When a solute molecule is at or near the illuminated surface and within a finite surface region under observation, it is excited by the evanescent field and fluorescence is detected; when the molecule either detaches from the surface or surface diffuses away from the observed region, no fluorescence from the molecule is detected. In typical experiments, most solute molecules within the evanescent field are those actually bound to the surface. Thus, measured fluorescence is due mainly to the surface bound solute molecules which are within a well-defined surface area.

In TIR/FPR experiments, the finite observation area is defined by focusing the totally internally reflected laser beam. The beam is flashed brightly in a single short pulse, thereby photobleaching the fluorescence of surface bound solute molecules in the region of the evanescent field. Subsequent fluorescence recovery is monitored by the same (but much attenuated) evanescent field, as bleached molecules exchange with chemically identical but unbleached molecules from solution and the surrounding nonilluminated regions of the surface. In TIR/FCS experiments, the laser beam may be unfocused and no bleaching pulse is employed. One observes the spontaneous fluctuations of fluorescence due to individual molecules entering and leaving a portion of the evanescent field defined by an aperture in an image plane of the fluorescence detection optical system. The average rate of decay of these fluctuations, which depends on the rates of surface adsorption and desorption and surface diffusion, is measured by autocorrelating the fluctuations from the equilibrium value of fluorescence.

We calculate the theoretical expressions for the TIR/FPR recovery curve and the TIR/FCS autocorrelation function. When cast in the proper mathematical form, the theoretical treatments of TIR/FPR and TIR/FCS are identical. The shape and characteristic time of experimentally obtained curves depend on the bulk and surface diffusion coefficients of the solute molecules, the size and shape of the observed region, and the surface adsorption and desorption rate constants. In appropriate limits, the adsorption/desorption rate constants and surface diffusion coefficients can be readily obtained. A discussion of experimental considerations and an experimental application of this new technique is presented in the accompanying paper (26).

DEFINITIONS

We consider molecules of bulk concentration $A(\mathbf{r}, z, t)$ freely diffusing in solution and reacting with free binding sites of surface concentration $B(\mathbf{r}, t)$ to form fluorescent complexes of surface concentration $C(\mathbf{r}, t)$. The reaction is represented by the chemical equation:

$$A(\mathbf{r}, z, t) + B(\mathbf{r}, t) \underset{k_2}{\overset{k_1}{\rightleftharpoons}} C(\mathbf{r}, t). \tag{1}$$

As illustrated in Fig. 1, vector $\mathbf{r}$ is the position on the surface measured from the center of the observation area, z is the perpendicular distance from the surface to a point in the solution, and t is the time. Parameters k_1 and k_2 are surface adsorption and desorption rate constants. The equilibrium constant of the reaction is κ, where

$$\kappa = \overline{C}/\overline{A}\overline{B} = k_1/k_2. \tag{2}$$

$\overline{C}$, $\overline{A}$, and $\overline{B}$ are equilibrium concentration values, and are independent of position (assuming surface homogeneity).

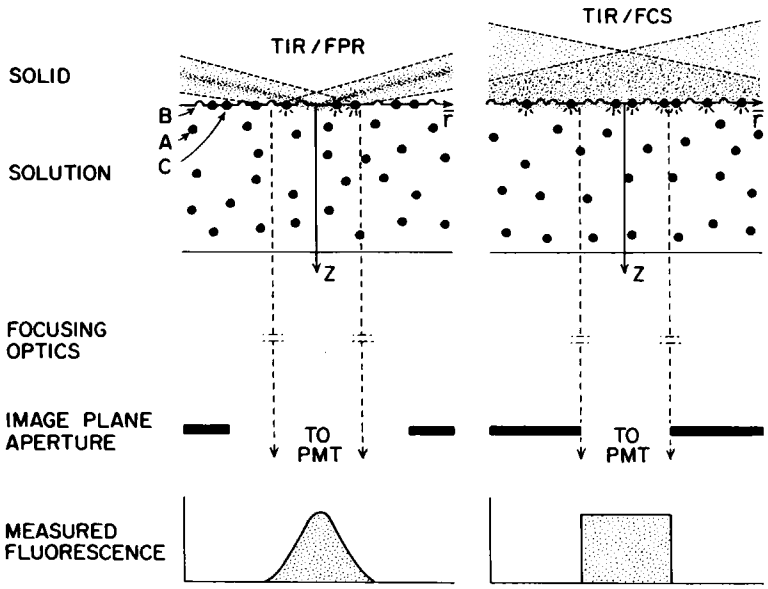

FIGURE 1 Schematic drawing of optical systems for TIR/FPR and TIR/FCS. A Gaussian laser beam either focused (TIR/FPR) or unfocused (TIR/FCS) at a totally internally reflecting solid/solution interface, creates a shallow evanescent field in the solution. Fluorescent solute molecules A (filled circles) are in equilibrium with the solid surface containing both free binding sites B (open hemicircles) and occupied binding sites C (hemicircles containing filled circles). Fluorescence is emitted only from bound solute molecules C excited by the evanescent field. Fluorescence is detected by a photomultiplier from a well-defined area on the surface. In TIR/FPR, the area is defined by the small lateral extent of the evanescent field. In TIR/FCS, the area is defined by an aperture placed at an image plane of the microscope. The aperture may be a clear hole in an opaque barrier, or it may be a film image of graded transmittivity (e.g., in the profile of a circular Gaussian). Position vector $\mathbf{r}$ lies in the plane of the solid/solution interface with origin at the center of the observation area, and z is the perpendicular to this plane.

We assume that each molecule within the evanescent field is bound to a surface site (see reference 26, Appendix A). The evanescent intensity $I(\mathbf{r})$ at the surface as viewed through the image plane aperture can be written as

$$I(\mathbf{r}) = I_0 \mathcal{I}(\mathbf{r}), \tag{3}$$

where I_0 is the maximum intensity and $\mathcal{I}(\mathbf{r})$ is a unitless profile function with unity maximum amplitude. For typical TIR/FPR experiments, $I(\mathbf{r})$ is the profile formed by the focused laser beam. For typical TIR/FCS experiments, $I(\mathbf{r})$ is the transmission function of the image plane aperture (see Fig. 1). The measured fluorescence $F(t)$ is then

$$F(t) = QI_0 \int \mathcal{I}(\mathbf{r}) C(\mathbf{r}, t) \mathrm{d}^2 r, \tag{4}$$

where Q is a product of the efficiencies of excitation light absorption and fluorescence emission and detection.

TIR/FPR

For TIR/FPR experiments, we solve for the monotonically decreasing function

$$G_p(t) = \overline{F} - F(t), \tag{5}$$

where $F(t)$ is the fluorescence after a photobleaching flash at $t = 0$ due to unbleached fluorophore within the observation region; $\overline{F}$ is the equilibrium prebleach fluorescence (and the fluorescence after complete recovery); and the subscript p denotes photobleaching experiments. We define

$$\begin{aligned} \mathcal{A}_p(\mathbf{r}, z, t) &= \overline{A} - A(\mathbf{r}, z, t) \\ \mathcal{C}_p(\mathbf{r}, t) &= \overline{C} - C(\mathbf{r}, t), \end{aligned} \tag{6}$$

where $\overline{A}$ and $\overline{C}$ are the equilibrium values of the bulk and surface concentrations of solute molecules (unbleached plus bleached), respectively. $\mathcal{A}(\mathbf{r}, z, t)$ and $\mathcal{C}(\mathbf{r}, t)$ are the bulk and surface concentrations of unbleached fluorescent solute molecules after the photobleaching flash at $t = 0$. Combining Eqs. 4, 5, and 6 yields

$$G_p(t) = QI_0 \int \mathcal{I}(\mathbf{r}) \mathcal{C}_p(\mathbf{r}, t) \mathrm{d}^2 r. \tag{7}$$

TIR/FCS

For TIR/FCS experiments, we solve for the autocorrelation function

$$G_c(t) = \langle \delta F(t) \delta F(0) \rangle, \tag{8}$$

where $\delta F(t) = F(t) - \overline{F}$. $\delta F(t)$ is the spontaneous fluctuation of fluorescence $F(t)$ at time t away from the mean fluorescence $\overline{F}$; time zero is arbitrary; the brackets represent a thermodynamic ensemble average; and the subscript c denotes correlation experiments.

The fluctuations of the three chemical species A, B, and C from their equilibrium concentrations $\overline{A}$, $\overline{B}$, and $\overline{C}$ are δA, δB, and δC, respectively. We define $\mathcal{A}_c$ and $\mathcal{C}_c$ to be the average correlations of a concentration fluctuation in A at $(\mathbf{r}, z)$ and C at $(\mathbf{r})$, respectively,

with a concentration fluctuation in C at $(\mathbf{r}')$, where the two fluctuations are separated by a time t:

$$\mathcal{A}_c(\mathbf{r}, \mathbf{r}', z, t) = \langle \delta A(\mathbf{r}, z, t) \delta C(\mathbf{r}', 0) \rangle$$

$$\mathcal{C}_c(\mathbf{r}, \mathbf{r}', t) = \langle \delta C(\mathbf{r}, t) \delta C(\mathbf{r}', 0) \rangle. \tag{9}$$

Combining Eqs. 4, 8, and 9 yields

$$G_c(t) = Q^2 I_0^2 \int \int \mathcal{I}(\mathbf{r})\, \mathcal{I}(\mathbf{r}') \mathcal{C}_c(\mathbf{r}, \mathbf{r}', t) \mathrm{d}^2 r \mathrm{d}^2 r'. \tag{10}$$

DIFFERENTIAL EQUATIONS

To solve for $G(t)$, we begin with the differential equations governing $A(\mathbf{r}, z, t)$ and $C(\mathbf{r}, t)$:[1]

$$\frac{\partial A}{\partial t} = D_A \nabla^2_{\mathbf{r},z} A$$

$$\frac{\partial C}{\partial t} = D_C \nabla^2_{\mathbf{r}} C + k_1 A_{z\to 0} B - k_2 C, \tag{11}$$

where D_A and D_C are the bulk and surface diffusion coefficients of the solute molecules and $A_{z\to 0} \equiv \lim_{z\to 0} A(\mathbf{r}, z, t)$. Note that the rate of change of surface concentration depends on the local bulk concentration A only at the $z = 0$ surface. Operators $\nabla^2_{\mathbf{r}}$ and $\nabla^2_{\mathbf{r},z}$ are two and three dimensional Laplacians, respectively.

The number of adsorptions per area per time and desorptions per area per time are $k_1 A_{z\to 0} B$ and $k_2 C$, respectively. The net flux of molecules to the surface from the solution is the difference between these two terms, and is equal to $D_A(\partial A/\partial z)_{z\to 0}$ (according to Fick's Law). Therefore, we obtain a boundary condition:

$$D_A \left(\frac{\partial A}{\partial z}\right)_{z\to 0} = k_1 A_{z\to 0} B - k_2 C. \tag{12}$$

To solve for both $G_p(t)$ and $G_c(t)$ concurrently, Eqs. 11 and 12 must be transformed into equations describing the variables $\mathcal{A}_p, \mathcal{C}_p$ and $\mathcal{A}_c, \mathcal{C}_c$.

TIR/FPR

We substitute expressions for A and C in terms of $\mathcal{A}$, $\mathcal{C}$, $\overline{A}$, and $\overline{C}$ (Eq. 6 into Eqs. 11 and 12) and use the equilibrium relationship Eq. 2. Although the relative concentration of bleached vs. unbleached fluorophore adsorbed to the surface changes with time during TIR/FPR recovery, the concentration of free binding sites remains constant at the equilibrium value $\overline{B}$ during fluorescence recovery. $B(\mathbf{r}, t)$ in Eqs. (11, 12) is therefore replaced by $\overline{B}$.

---

[1]For TIR/FPR, the variables A, B, and C implicitly denote time- and space-dependent ensemble averages over many macroscopically identical systems. The average response of the system to a microscopic perturbation (e.g., a spontaneous concentration fluctuation) and its response to a macroscopic perturbation (e.g., photobleaching) are both governed by the same equations.

TIR/FCS

We write A, B, and C in terms of $\bar{A}$, $\bar{B}$, $\bar{C}$, δA, δB, and δC, and substitute these expressions into Eqs. 11 and 12. The total concentration of surface sites (free sites B plus bound sites C) remains exactly constant during an experiment; thus $\delta B = -\delta C$. After applying the equilibrium relationship Eq. 2, and eliminating a term proportional to the product of two fluctuations, we multiply the resultant equations by $\delta C(\mathbf{r}', 0)$ and take the thermodynamic ensemble average on both sides of each equation.

The resulting differential equations for TIR/FPR and TIR/FCS are formally identical, as follows (with subscripts p and c suppressed):

$$\frac{\partial \mathcal{A}}{\partial t} = D_A \nabla^2_{r,z} \mathcal{A}$$

$$\frac{\partial \mathcal{C}}{\partial t} = D_C \nabla^2_r C + k_1 \bar{B} \mathcal{A}_{z\to 0} - R_R \mathcal{C}$$

$$D_A \left(\frac{\partial \mathcal{A}}{\partial z}\right)_{z\to 0} = k_1 \bar{B} \mathcal{A}_{z\to 0} - R_R \mathcal{C}, \tag{13}$$

where

$$R_R \equiv \begin{cases} k_2 & \text{for TIR/FPR} \\ k_1 \bar{A} + k_2 & \text{for TIR/FCS.} \end{cases} \tag{14}$$

The subscript R (for reaction) denotes the dependence of the rate on the adsorption/desorption reaction kinetics. One of the goals of TIR/FPR and TIR/FCS experiments is to measure R_R.

BOUNDARY AND INITIAL CONDITIONS

The boundary and initial conditions for $\mathcal{A}_p$ and $\mathcal{C}_p$ are similar to those for $\mathcal{A}_c$ and $\mathcal{C}_c$.

TIR/FPR

In TIR/FPR, only the surface bound molecules within a finite surface area are photobleached, so that $C(\mathbf{r}, t)$ and $A(\mathbf{r}, z, t)$ far away from the bleached region never depart from the equilibrium values $\bar{C}$ and $\bar{A}$, respectively, during fluorescence recovery:

$$[\mathcal{C}_p(\mathbf{r}, t)]_{|\mathbf{r}|\to\infty} = [\mathcal{A}_p(\mathbf{r}, z, t)]_{|\mathbf{r}|\to\infty} = 0 \tag{15}$$

$$[\mathcal{A}_p(\mathbf{r}, z, t)]_{z\to\infty} = 0. \tag{16}$$

Immediately after bleaching surface bound fluorophore at time $t = 0$, the unbleached bulk concentration $[A(\mathbf{r}, z, t)]_{t\to 0}$ is equal to $\bar{A}$:

$$[\mathcal{A}_p(\mathbf{r}, z, t)]_{t\to 0} = 0. \tag{17}$$

The concentration $[C(\mathbf{r}, t)]_{t\to 0}$ of unbleached fluorophore on the surface (for a short bleaching pulse) is a function of the laser intensity profile, so that (reference 19, p. 1,056):

$$[\mathcal{C}_p(\mathbf{r}, t)]_{t\to 0} = \bar{C}(1 - e^{-K\mathcal{I}(\mathbf{r})}), \tag{18}$$

where K is a product of the intrinsic bleaching efficiency of the fluorophore and the bleaching duration and power. Using Eqs. 7 and 18, the initial value of $G_p(t)$ is

$$G_p(0) = \bar{C}QI_0 \int \mathcal{J}(\mathbf{r})[1 - e^{-K\mathcal{J}(\mathbf{r})}]\mathrm{d}^2r. \tag{19}$$

TIR/FCS

In TIR/FCS, the correlation between concentration fluctuations at two positions infinitely separated in space must be equal to zero, so that

$$[\mathcal{C}_c(\mathbf{r}, \mathbf{r}', t)]_{|\mathbf{r}-\mathbf{r}'|\to\infty} = [\mathcal{A}_c(\mathbf{r}, \mathbf{r}', z, t)]_{|\mathbf{r}-\mathbf{r}'|\to\infty} = 0 \tag{20}$$

$$[\mathcal{A}_c(\mathbf{r}, \mathbf{r}', z, t)]_{z\to\infty} = 0. \tag{21}$$

Concentration $A(\mathbf{r})$ is defined within a small subvolume at location $\mathbf{r}$. This subvolume is open to an infinite reservoir of molecules in the bulk solution. The subvolume thereby contains a variable number of molecules which follows a Poisson distribution. A concentration fluctuation δA from equilibrium in the subvolume is uncorrelated with a concentration fluctuation δC on the surface at the same time (20):[2]

$$[\mathcal{A}_c(\mathbf{r}, \mathbf{r}', z, t)]_{t\to 0} = 0. \tag{22}$$

(Note, however, that a fluctuation in A can be correlated with a fluctuation in C at a different time.) For a finite number of surface binding sites, the average of the square of the number fluctuation of adsorbed solute molecules within the observation region is equal to the product of the mean number of adsorbed molecules in this area and the average fraction β of the binding sites which are free (27), so that

$$[\mathcal{C}_c(\mathbf{r}, \mathbf{r}', t)]_{t\to 0} = \beta\bar{C}\delta(\mathbf{r} - \mathbf{r}'), \tag{23}$$

where

$$\beta = \bar{B}/(\bar{B} + \bar{C}). \tag{24}$$

Using Eqs. 10 and 23, the initial value of $G_c(t)$ is

$$G_c(0) = \beta\bar{C}Q^2I_0^2 \int \mathcal{J}^2(\mathbf{r})\mathrm{d}^2r. \tag{25}$$

SOLUTION FOR $G(t)$

Eq. 13 can be solved by linear transformation theory. We Fourier transform with respect to the surface position vector ($\mathbf{r}\to\mathbf{q}$) and Laplace transform with respect to the normal to the surface ($z\to p$) and time ($t\to\omega$). In the following, transformations which have been performed are indicated solely by the variables in parentheses after the symbol $\mathcal{A}$ or $\mathcal{C}$.

The transformed states of Eq. 13 together with the boundary and initial conditions Eqs. 15,

[2]This statement assumes that, in each observation region, the number of solute molecules whose positions are correlated by steric hindrance, van der Waal's attraction, electrostatic interaction, etc., is negligible compared to the number of independently acting solute molecules. To first order, actual deviations from this approximation would be expressed as altered phenomenological coefficients for reaction kinetics and diffusion.

17 and 20, 22 are

$$\frac{\omega}{D_A}\mathcal{A}(\mathbf{q}, p, \omega) = (p^2 - q^2)\mathcal{A}(\mathbf{q}, p, \omega) - p[\mathcal{A}(\mathbf{q}, z, \omega)]_{z\to 0} - \left[\frac{\partial \mathcal{A}}{\partial z}(\mathbf{q}, z, \omega)\right]_{z\to 0} \quad (26)$$

$$\omega \mathcal{C}(\mathbf{q}, \omega) - [\mathcal{C}(\mathbf{q}, t)]_{t\to 0} = -D_C q^2 \mathcal{C}(\mathbf{q}, \omega) + k_1 \bar{B}[\mathcal{A}(\mathbf{q}, z, \omega)]_{z\to 0} - R_R \mathcal{C}(\mathbf{q}, \omega) \quad (27)$$

$$D_A\left[\frac{\partial \mathcal{A}}{\partial z}(\mathbf{q}, z, \omega)\right]_{z\to 0} = k_1 \bar{B}[\mathcal{A}(\mathbf{q}, z, \omega)]_{z\to 0} - R_r \mathcal{C}(\mathbf{q}, \omega). \quad (28)$$

Solving Eq. 26 for $\mathcal{A}(\mathbf{q}, p, \omega)$ and inverse Laplace transforming from p-space back to z-space (28), yields

$$\mathcal{A}(\mathbf{q}, z, \omega) =$$

$$\tfrac{1}{2}\left\{[\mathcal{A}(\mathbf{q}, z, \omega)]_{z\to 0} + (q^2 + \omega/D_A)^{-1/2}\left[\frac{\partial \mathcal{A}}{\partial z}(\mathbf{q}, z, \omega)\right]_{z\to 0}\right\} \exp\left[(q^2 + \omega/D_A)^{1/2} z\right]$$

$$+ \tfrac{1}{2}\left\{[\mathcal{A}(\mathbf{q}, z, \omega)]_{z\to 0} - (q^2 + \omega/D_A)^{-1/2}\left[\frac{\partial \mathcal{A}}{\partial z}(\mathbf{q}, z, \omega)\right]_{z\to 0}\right\} \exp\left[-(q^2 + \omega/D_A)^{1/2} z\right]. \quad (29)$$

We choose $Re\,[q^2 + \omega/D_A] \geq 0$ and apply the boundary conditions on $\mathcal{A}$ as $z \to \infty$ (Eqs. 16 and 21), which then requires that

$$[\mathcal{A}(\mathbf{q}, z, \omega)]_{z\to 0} = -(q^2 + \omega/D_A)^{-1/2}\left[\frac{\partial \mathcal{A}}{\partial z}(\mathbf{q}, z, \omega)\right]_{z\to 0}. \quad (30)$$

Eq. 30 together with Eq. 28 yields a solution for $[\mathcal{A}(\mathbf{q}, z, \omega)]_{z\to 0}$ in terms of $\mathcal{C}(\mathbf{q}, \omega)$. This is substituted into Eq. 27 to arrive at a solution for $\mathcal{C}(\mathbf{q}, \omega)$:

$$\mathcal{C}(\mathbf{q}, \omega) = N(q, \omega)[\mathcal{C}(\mathbf{q}, t)]_{t\to 0}, \quad (31)$$

where

$$N(q, \omega) = \frac{\sqrt{q^2 D_A + \omega} + k_1 \bar{B}/\sqrt{D_A}}{(\omega + R_R + q^2 D_C)\sqrt{q^2 D_A + \omega} + (\omega + q^2 D_C) k_1 \bar{B}/\sqrt{D_A}}. \quad (32)$$

To arrive at $G_p(t)$ and $G_c(t)$, we put Eq. 31 together with the initial conditions Eqs. 18 and 23 into Eqs. 7 and 10, thereby obtaining

$$G_p(t) = QI_0 \int \mathcal{I}(\mathbf{r}) L^{-1}_{\omega\to t} F^{-1}_{\mathbf{q}\to \mathbf{r}} \{N(q, \omega) F_{\mathbf{r}'\to \mathbf{q}} [\bar{C}(1 - e^{-K\mathcal{I}(\mathbf{r}')})]\}\, d^2 r, \quad (33)$$

and

$$G_c(t) = Q^2 I_0^2 \int\int \mathcal{I}(\mathbf{r})\mathcal{I}(\mathbf{r}') L^{-1}_{\omega\to t} F^{-1}_{\mathbf{q}\to \mathbf{r}} [N(q, \omega) F_{\mathbf{r}'\to \mathbf{q}} \{\beta \bar{C}\delta(\mathbf{r}' - \mathbf{r}'')\}] d^2 r d^2 r', \quad (34)$$

where F refers to Fourier transform, and F^{-1} and L^{-1} refer to inverse Fourier and Laplace transforms. Apart from multiplicative constants, $G_p(t)$ is identical to $G_c(t)$ in the limit of shallow photobleaching, $K \ll 1$. Referring to the expressions for the initial values of $G_p(t)$ and $G_c(t)$ (Eqs. 19 and 25), and applying Parseval's theorem, we rewrite $G(t)$ as

$$G(t) = G(0) L^{-1}_{\omega\to t} \int |\mathcal{I}(\mathbf{q})|^2 N(q, \omega) d^2 q \Big/ \int |\mathcal{I}(\mathbf{q})|^2 d^2 q, \quad (35)$$

where $\mathcal{I}(\mathbf{q})$ is the Fourier transform of $\mathcal{I}(\mathbf{r})$. Eq. 35 is true for TIR/FCS in general and for TIR/FPR when $K \ll 1$.

CHARACTERISTIC RATES

We wish to recast $G(t)$ in terms of physically significant characteristic rate parameters whose relative sizes determine the shape of $G(t)$. The form of the characteristic rate parameters can be obtained by converting the arguments $\mathbf{q}$ and ω in the integrand of Eq. 35 to unitless variables $\boldsymbol{\xi}$ and ν, as follows. We rewrite $\mathcal{I}(\mathbf{r})$ quite generally with unitless argument as

$$\mathcal{I}(\mathbf{r}) = \frac{1}{s^2}\mathcal{I}'(\mathbf{r}/s), \tag{36}$$

where s is a characteristic linear dimension of the observed region and $\mathcal{I}'(\mathbf{r}/s)$ is an intensity profile function with unitless argument. Then, the Fourier transform of Eq. 36 is

$$\mathcal{I}(\mathbf{q}) = \mathcal{I}'(\boldsymbol{\xi}), \tag{37}$$

where $\boldsymbol{\xi} \equiv \mathbf{q}s$ and $\mathcal{I}'(\boldsymbol{\xi})$ is the Fourier transform of $\mathcal{I}'(\mathbf{r}/s)$. In addition, we define $\nu \equiv \omega/R_R$. From Eqs. 2, 32, 35 and 37, we obtain

$$G(t) = G(0)\,L^{-1}_{\nu \to R_R t} \int |\mathcal{I}'(\boldsymbol{\xi})|^2 N(\xi, \nu) \mathrm{d}^2\xi \Big/ \int |\mathcal{I}'(\boldsymbol{\xi})|^2 \mathrm{d}^2\xi, \tag{38}$$

where

$$N(\xi, \nu) = \frac{(\nu + \xi^2 R_{\mathrm{BLD}}/R_R)^{1/2} + (R_R/R_{\mathrm{BND}})^{1/2}}{(1 + \nu + \xi^2 R_{\mathrm{SD}}/R_R)(\nu + \xi^2 R_{\mathrm{BLD}}/R_R)^{1/2} + (\nu + \xi^2 R_{\mathrm{SD}}/R_R)(R_R/R_{\mathrm{BND}})^{1/2}}, \tag{39}$$

and

$$\begin{aligned}
R_R &\equiv \begin{matrix} k_2 & \text{for TIR/FPR} \\ k_1\bar{A} + k_2 & \text{for TIR/FCS} \end{matrix} && \text{reaction rate} \\
R_{\mathrm{BND}} &\equiv \begin{matrix} D_A/(\bar{C}/\bar{A})^2 & \text{for TIR/FPR} \\ D_A/(\beta\bar{C}/\bar{A})^2 & \text{for TIR/FCS} \end{matrix} && \text{bulk normal diffusion rate} \\
R_{\mathrm{BLD}} &\equiv D_A/s^2 && \text{bulk lateral diffusion rate} \\
R_{\mathrm{SD}} &\equiv D_C/s^2 && \text{surface diffusion rate}
\end{aligned} \tag{40}$$

These four parameters are characteristic rates which describe distinct physical processes. Because of the complexity of Eqs. 38 and 39, we present here a qualitative discussion of the expected behavior of $G(t)$ in terms of its characteristic rates, before resuming a more formal development in the next section.

R_R

To explain the significance of R_R, we consider a very large observation area ($s \to \infty$), so that diffusion rates parallel to the surface (R_{BLD}, R_{SD}) are negligibly small. We also assume that diffusion in the bulk is very fast (characterized by a large D_A). In TIR/FPR, as adsorbed bleached molecules desorb, they quickly diffuse away from the region near the surface (Fig.

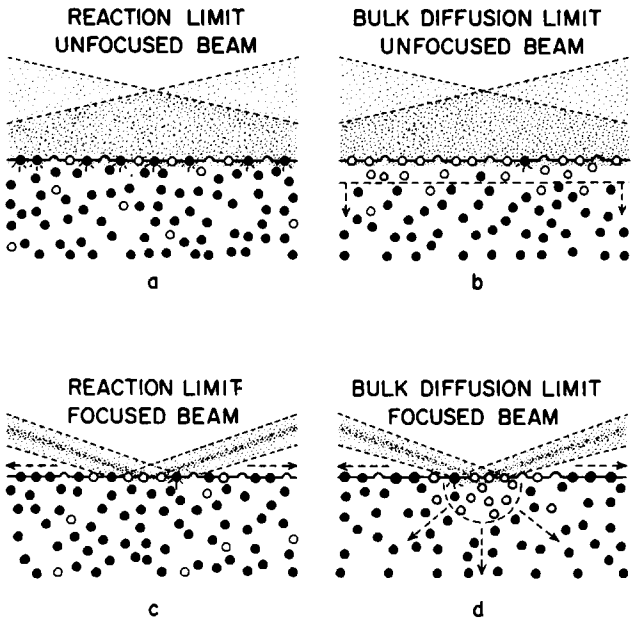

FIGURE 2 Conceptual illustration of surface kinetics. The reaction limit vs. bulk diffusion limit is shown with particular reference to TIR/FPR. The concentrations of bleached (open circles) vs. unbleached (filled circles) as a function of position are depicted schematically at a short time after photobleaching. We assume the same kinetic constants k_1 and k_2 and the same time t after photobleaching in each panel (*a–d*); only bulk diffusion constant D_A and observation size s are varied. (*a*) Reaction limit, $s \rightarrow \infty$. The bleached solute has diffused far from the surface and has become diluted uniformly in the bulk solution. (*b*) Bulk diffusion limit, $s \rightarrow \infty$. The bleached solute remains in a "cloud" near the surface. The slow diffusive dispersal of the cloud (shown bordered by a dotted line) limits the rate of fluorescence recovery. (*c*) Reaction limit, s finite. The bleached solute rapidly becomes diluted uniformly in the bulk solution, as in *a*; surface diffusion provides a parallel route for fluorescence recovery. (*d*) Bulk diffusion limit, s finite. The diffusive dispersal of the cloud of bleached solute in the bulk limits the fluorescence recovery rate, as in *b*; however, the cloud can disperse more rapidly due to the three-dimensional mode of escape. Surface diffusion will speed the recovery as well as alter the shape of the bleached cloud.

2 *a*). The probability of a desorbed bleached molecule readsorbing to the surface during the time course of the experiment is very small. The system is analogous to a unimolecular isomerization reaction between adsorbed (C) and desorbed (A) unbleached solute molecules, where the number of A molecules is very large and behaves as an infinite reservoir to C molecules. The relaxation rate of this reaction (and thus the rate of fluorescence recovery) is k_2, which is just R_R for TIR/FPR. In TIR/FCS, a surface concentration fluctuation relaxes by adsorption/desorption, becoming a bulk concentration fluctuation which quickly diffuses away from the surface. Because the total number of binding sites ($B + C$) remains constant during the relaxation process, this system is analogous to a unimolecular isomerization reaction between bound (C) and unbound (B) sites on the surface. The relaxation rate of this reaction (and thus the average rate of relaxation of fluctuations) is $k_1\bar{A} + k_2$, which is just R_R for TIR/FCS. For both TIR/FPR and TIR/FCS, we expect $G(t)$ to decay with characteristic rate R_R. This case of fast bulk diffusion and relatively slow adsorption/desorption is called the "reaction limit."

R_{BND}

At the other extreme from the reaction limit, bulk diffusion is slow. For TIR/FPR, in this case, adsorbed bleached molecules diffuse only very slowly from the vicinity of the bleached surface after desorption, resulting in a long-lived "cloud" of bleached solute immediately adjacent to the surface (Fig. 2 *b*). Some of the bleached solute will readsorb to the surface, thereby slowing the fluorescence recovery. The rate of recovery is no longer governed by the desorption rate k_2, but instead by the bulk diffusion coefficient D_A. The characteristic rate is determined by how rapidly bleached molecules on the surface can be completely replaced by an equal number of unbleached molecules from the bulk. For a (large) surface area S, the number of molecules on the surface is $\overline{C}S$; an equal number $\overline{A}S\ell_p$ will be found within some characteristic distance ℓ_p from the surface when $\ell_p = \overline{C}/\overline{A}$. Characteristic rate R_{BND} for TIR/FPR then becomes D_A/ℓ_p^2.

In TIR/FCS, length ℓ_c is determined by how rapidly a surface concentration fluctuation in C relaxes through exchange with a bulk concentration fluctuation in A. Consider, as above, a volume defined by a given surface area extended into the solution a distance ℓ_c. Because this volume is open to transport of solute molecules, the average number fluctuation of A at equilibrium is given by $\langle \delta N_A^2 \rangle = \langle N_A \rangle = \overline{A}S\ell_c$. Because the total number of binding sites is finite, the average number fluctuation of C at equilibrium is given by $\langle \delta N_C^2 \rangle = \beta \langle N_C \rangle = \beta\overline{C}S$ (27). The length ℓ_c for which the average number fluctuation of solute molecules $\langle \delta N_A^2 \rangle$ is equal to the average number fluctuation of surface bound molecules $\langle \delta N_c^2 \rangle$ is calculated from $\beta\overline{C}S = \overline{A}S\ell_c$, which gives $\ell_c = \beta\overline{C}/\overline{A}$. Characteristic rate R_{BND} for TIR/FCS then becomes D_A/ℓ_c^2.

For both TIR/FPR and TIR/FCS, R_{BND} can thus be interpreted as the bulk diffusion rate normal to the surface across a depth of solution ℓ. When bulk diffusion across ℓ is slow, R_{BND} determines the decay rate of $G(t)$. This situation is called the "bulk diffusion limit." In this limit, $G(t)$ becomes sensitive to bulk solution properties (D_A and $\overline{A}$) rather than to surface reaction rate R_R.

R_{SD}

R_{SD} is the rate of surface diffusion (with coefficient D_C) through an area with a finite characteristic length s. In general, surface diffusion speeds the decay of $G(t)$.

R_{BLD}

R_{BLD} is the rate by which already desorbed molecules can exit the vicinity of the surface observation area by lateral diffusion in the bulk (i.e., parallel rather than normal to the surface). An increasing R_{BLD} (due to $s \rightarrow 0$) allows for faster dissipation of the "cloud" of bleached solute (for TIR/FPR, see Fig. 2 *c* and *d*) or concentration fluctuation (for TIR/FCS) in the vicinity of the observed region. This effect tends to bring $G(t)$ farther from the bulk diffusion limit and closer to the reaction limit.

LIMITING SOLUTIONS

In this section, we rigorously examine the limit behavior of $G(t)$ as characteristic rate ratios are varied. In some experimentally attainable limits, $G(t)$ assumes simple and useful explicit forms; in instructive intermediate cases, $G(t)$ curves are computer-generated.

Very Large Observation Area: $s \to \infty$

We can obtain an analytic solution for $G(t)$ when the characteristic length s of the illuminated and observed area is very large. In this case, the diffusion rates parallel to the surface observation area (R_{BLD}, R_{SD}) are negligibly small. The factors determining $G(t)$ are the reaction rate R_R and the net z-direction diffusion rate R_{BND}. Upon rewriting for $s \to \infty$, Eqs. 38 and 39 can be expressed as a sum of four partial fractions which can be readily inverse Laplace transformed (28) to obtain the following real function:

$$G(t) = \frac{G(0)}{\nu_-^{1/2} - \nu_+^{1/2}} [\nu_-^{1/2} w(-i\sqrt{\nu_+ R_R t}) - \nu_+^{1/2} w(-i\sqrt{\nu_- R_R t})], \tag{41}$$

where

$$\nu_\pm^{1/2} = \tfrac{1}{2}\sqrt{\frac{R_R}{R_{BND}}}\{-1 \pm \sqrt{1 - 4R_{BND}/R_R}\}; \tag{42}$$

and

$$w(i\eta) = e^{\eta^2} \operatorname{erfc}(\eta) \quad (\eta \text{ complex}). \tag{43}$$

Unlike Eq. 38, Eq. 41 is valid for all K values in TIR/FPR. This solution for $G(t)$ can also be obtained directly from differential equations containing no surface position dependence (i.e., in Eq. 11 set $\nabla_r^2 C = 0$, and $\nabla_{r,z}^2 A = \partial^2 A/\partial z^2$). $G(t)$ is graphed in Fig. 3 for several values of the ratio R_R/R_{BND}. The extremes of R_R/R_{BND} lead to simple analytic forms of $G(t)$, discussed as follows.

REACTION LIMIT: $R_R/R_{BND} \to 0$; $R_{BLD} = R_{SD} = 0$ If the reaction rate R_R is much smaller than the bulk normal diffusion rate R_{BND}, $G(t)$ depends only on R_R. This is the ideal

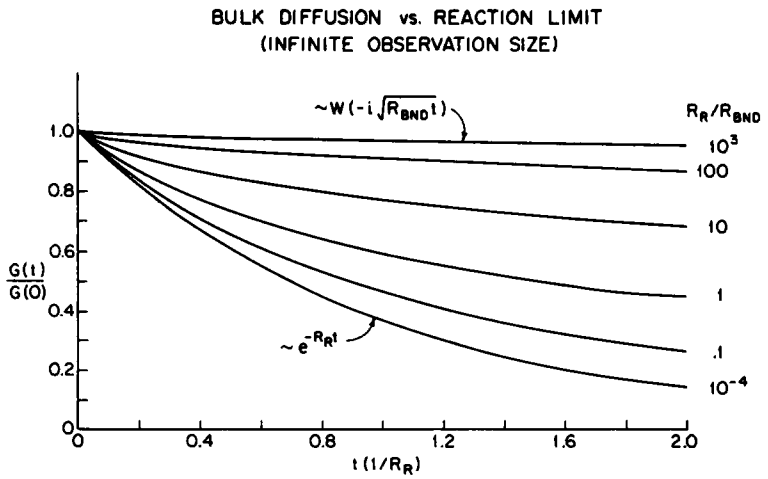

FIGURE 3 $G(t)$ for very large observation area ($s \to \infty$) and variable ratio R_R/R_{BND}. As $R_R/R_{BND} \to 0$ (reaction limit), $G(t) \to G(0) \exp(-R_R t)$. As $R_R/R_{BND} \to \infty$ (bulk diffusion limit), $G(t) \to G(0)\, w(-i\sqrt{R_{BND} t})$. Time is plotted in units of $1/R_R$. The normalized initial slope is always $-R_R$.

state for measuring surface kinetic rates. In this case, $\nu_{\pm}^{1/2}$ approach $\pm i$. Using a mathematical identity involving w-functions (28), we find that Eq. 41 approaches

$$G(t) \simeq G(0)e^{-R_R t}. \tag{44}$$

BULK DIFFUSION LIMIT: $R_R/R_{BND} \to \infty$; $R_{BLD} = R_{SD} = 0$ For a fixed R_R and large observation area, decreasing the bulk diffusion rate R_{BND} can only lead to a slower decay of $G(t)$ than that given by Eq. 44. If the bulk normal diffusion rate R_{BND} is much smaller than the reaction rate R_R, $G(t)$ depends only on R_{BND}. Under these conditions, the time course of $G(t)$ is related to bulk diffusion, not to surface kinetics, and the rates k_1 and k_2 cannot be easily obtained. (This problem can sometimes be overcome, as discussed below.) As $R_R/R_{BND} \to \infty$, Eq. 41 approaches

$$G(t) \simeq G(0)w(-i\sqrt{R_{BND}t}). \tag{45}$$

Finite Observation Area

We have not obtained a general analytic solution for $G(t)$ in all cases of characteristic rate ratios for a finite observation area. However, in the reaction limit, a useful analytic function does exist. In all other cases, $G(t)$ curves are computer-generated.

To simplify the presentation, we discuss mainly the low bleach limit ($K \ll 1$) in TIR/FPR. In this limit, the shape of $G(t)$ is identical for both TIR/FPR and TIR/FCS. However, the recovery curves for the deeper bleaching used in practical FPR experiments (generally $K < 3$ for a Gaussian beam profile) deviate only slightly in shape and rate from those for $K \ll 1$ (18).

REACTION LIMIT WITH SURFACE DIFFUSION: $R_R/R_{BND} \to 0$ If the reaction rate R_R is much smaller than the bulk normal diffusion rate R_{BND}, $G(t)$ depends only on R_R and the surface diffusion rate R_{SD}, regardless of the size of the illuminated and observed area. Allowing $R_R/R_{BND} \to 0$ as R_{SD}/R_R remains finite[3] in Eqs. 38 and 39, inverse Laplace transforming, and applying Parseval's theorem and the convolution theorem, $G(t)$ can be rewritten in terms of real space variables[4] as

$$\frac{G(t)}{G(0)} = e^{-R_R t} \int\int \frac{\mathcal{I}(\mathbf{r})\mathcal{I}(\mathbf{r}')}{(4\pi D_C t)^{1/2}} \exp\left(-|\mathbf{r} - \mathbf{r}'|^2/4D_C t\right) d^2r d^2r' \Big/ \int \mathcal{I}^2(\mathbf{r}) d^2r. \tag{46}$$

Thus, $G(t)$ is the product of a simple exponential characteristic of the surface adsorption/desorption kinetics and a factor characteristic of surface diffusion through the observation area. Explicit forms of $G(t)$ for some intensity profiles likely to be encountered in practical experiments are shown in Table 1.

BULK DIFFUSION LIMIT AND INTERMEDIATE CASES: $R_R/R_{BND} \not\to 0$ We have not obtained analytical solutions for the finite surface area, nonreaction limit case. However, further development of Eqs. 38 and 39 leads to an appropriate form for computer-generation

[3]This method of approximation is not mathematically rigorous within the integral of Eq. 38. However, Eq. 46 can be derived exactly, assuming $[A(\mathbf{r}, z, t)]_{z\to 0} = \bar{A}$ (equivalent to assuming the reaction limit).

[4]Eq. 46 can be generalized to deeper bleaching (i.e., higher K) in TIR/FPR by replacing $\mathcal{I}(\mathbf{r})$, but not $\mathcal{I}(\mathbf{r}')$, with $K^{-1}(1 - e^{-K\mathcal{I}(\mathbf{r})})$.

TABLE I
REACTION LIMITED G(t) FOR COMMON INTENSITY PROFILES $\mathcal{I}(\mathbf{r})$

$\mathcal{I}(\mathbf{r})$	$G(t)/[G(0)\exp(-R_R t)]$	Comments
$e^{-2x^2/s^2}e^{-2\gamma^2y^2/s^2}$	$(1+4R_{SD}t)^{-1/2}(1+4\gamma R_{SD}t)^{-1/2}$	Elliptical Gaussian; formed by total internal internal reflection of circular Gaussian beam; useful for TIR/FPR.
e^{-2r^2/s^2}	$(1+4R_{SD}t)^{-1}$	Circular Gaussian; formed by suitable image plane transmission function; useful for TIR/FCS.
e^{-2x^2/s^2}	$(1+4R_{SD}t)^{-1/2}$	Linear Gaussian; approximates a profile encountered for TIR/FPR (see reference 26).
$1\begin{cases}\lvert x\rvert \le s/2\\ \lvert y\rvert \le s/2\end{cases}$	$\{\text{erf}\,[\frac{1}{2}(R_{SD}t)^{-1/2}]$ $+2(R_{SD}t/\pi)^{1/2}[\exp(-\frac{1}{4}R_{SD}t)-1]\}^2$	Square; formed by an image plane aperture useful for TIR/FCS.

$G(t)/G(0)$ is the product of $\exp(-R_R t)$ and a factor characteristic of surface diffusion through the observation area defined by $\mathcal{I}(\mathbf{r})$.

of $G(t)$ in these cases (see Appendix). These curves, displayed in Fig. 4 *a* and *b*, demonstrate the essential behavior of $G(t)$ as characteristic rate ratios are varied through intermediate cases.

Fig. 4 *a* shows that for a fixed finite s, the reaction limit can be approached as $R_R/R_{BND} \to 0$. In terms of experimental variables, R_R/R_{BND} may be decreased by increasing the bulk concentration A.

Fig. 4 *b* shows the effect of varying the size of the observation area. Given a $G(t)$ which is near the bulk diffusion limit at very large observation area, progressively reducing s causes $G(t)$ to approach the reaction limit. A $G(t)$ which is already in the reaction limit at large observation area will remain in the reaction limit as s is reduced.

EXPERIMENTAL ANALYSIS

In this section we discuss how to analyze an experimental $G(t)$ to extract the desired parameters k_1, k_2, and D_C.

Determining the Limiting Case

A key question is whether $G(t)$ is close to the reaction limit. In general, this question may be answered by curve-fitting experimental data to the various theoretical and computer-generated forms for $G(t)$ given in the above sections. The following approaches to the problem are simpler if less general.

We may attempt to compare the decay rate of an experimental $G(t)$ with the theoretical bulk diffusion limit rate R_{BND}. R_{BND} may be calculated directly from Eq. 40. To obtain an estimate of the experimental $G(t)$ decay rate, we measure time τ for $1/e$ decay. If $1/\tau \sim R_{BND}$, then $G(t)$ is near the bulk diffusion limit. But if $1/\tau \ll R_{BND}$, then $G(t)$ is near the reaction limit.

In TIR/FPR only, variation of $\bar{A}/\bar{C}$ affects R_{BND} but does not affect R_R. Therefore, a bulk

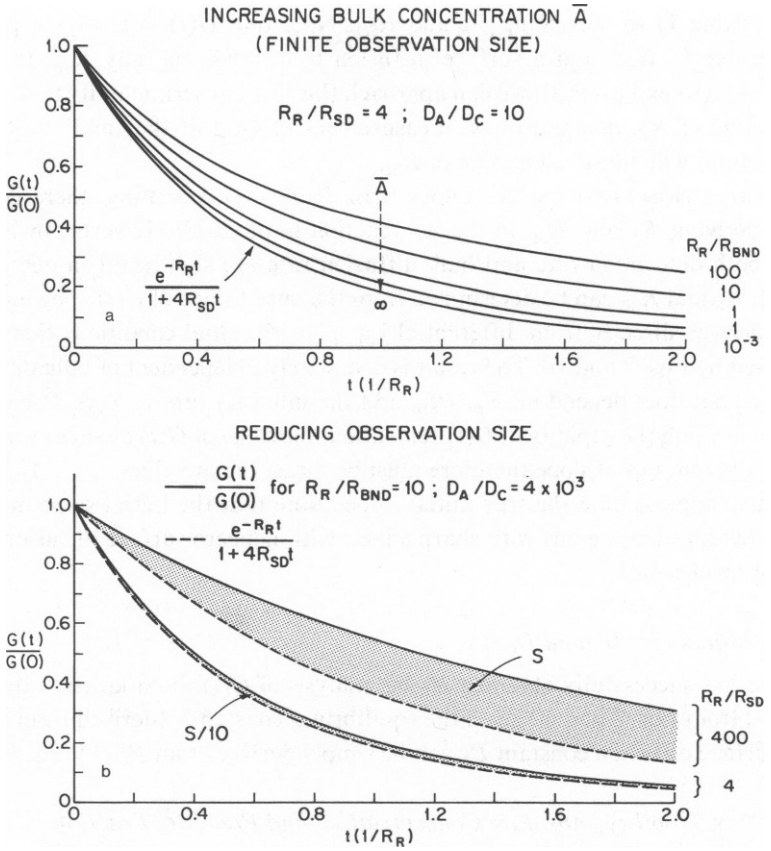

FIGURE 4 $G(t)$ for finite circular Gaussian observation area. $G(t)/G(0)$ is calculated by computer, as outlined in the Appendix. Time is plotted in units of $1/R_R$. (*a*) As concentration $\overline{A}$ is increased, $R_R/R_{BND} \rightarrow 0$, and $G(t) \rightarrow G(0) \exp(-R_R t)/(1 + 4R_{SD}t)$, regardless of the values of R_{SD} and R_{BLD}. Arbitrarily chosen are the relative rates $4R_{SD} = R_R$ and $4R_{BLD} = 10\ R_R$. (*b*) As the characteristic size of the observation area s is reduced, $R_R/R_{BLD} \rightarrow 0$, and $G(t) \rightarrow G(0) \exp(-R_R t)/(1 + 4R_{SD}t)$, regardless of the values of R_{SD} and R_{BND}. Arbitrarily chosen are the relative rates $4R_{SD} = 10^{-3}\ R_R$ and $R_{BND} = 0.1\ R_R$.

diffusion limited $G(t)$ will change its shape upon experimental variation of $\overline{A}/\overline{C}$ but a reaction limited $G(t)$ will not change its shape.

Forcing G(t) toward the Reaction Limit

Experimental increase of bulk concentration $\overline{A}$ or experimental reduction of observation region size s will always bring $G(t)$ closer to the reaction limit. However, concentration $\overline{A}$ should not be increased so far that the number of bulk solute molecules in the evanescent field is comparable to the number adsorbed to the surface; size s cannot be decreased to less than the optical resolution limit of the fluorescence detection system.

Obtaining Rates R_R and R_{SD} from G(t)

REACTION LIMIT Assuming we have confirmed that $G(t)$ is in the reaction limit as above, we may use the form of $G(t)$ appropriate to the known observation intensity profile

(Eq. 46 and Table 1) to determine R_R and R_{SD}. Note that $G(t)$ is always a product of a reaction term exp $(-R_R t)$ and a surface diffusion term involving only R_{SD}. In general, as $s \rightarrow \infty$, $G(t) \rightarrow G(0)$ exp $(-R_R t)$; we can approach this limit experimentally to determine R_R. Given knowledge of R_R, one additional measurement of $G(t)$ at the smallest s (limited by optical diffraction) will allow calculation of R_{SD}.

NONREACTION LIMIT CASES Other than detailed curve-fitting, there is no general approach to deriving R_R and R_{SD} in the nonreaction limit cases. However, in intermediate cases where both desorption rate and bulk diffusion rate are significant in determining the shape of $G(t)$, R_R and R_{SD} can be determined from the initial slope of $G(t)$. The initial slope of $G(t)$ can be derived directly from differential Eq. 13 with initial conditions Eqs. 17, 18, 22, and 23 followed by Eqs. 7 and 10. The result is completely independent of bulk diffusion rates R_{BND} and R_{BLD} but does depend on R_R, R_{SD}, and the intensity profile $\mathcal{I}(\mathbf{r})$. If bulk diffusion plays a role in limiting the rapidity of $G(t)$ relaxation, the slope of $G(t)$ changes very rapidly at small t. The apparent initial slope therefore must be measured at values of $t \ll 1/R_{BND}$ for the measurement to approximate the true initial slope. Note that the initial slope method is not applicable to observation regions with sharp edges; with nonzero surface diffusion, the initial slope then approaches infinity.

Determining k_1, k_2, and D_C

Assuming one has successfully obtained R_R by analysis of $G(t)$, both kinetic rates k_1 and k_2 can be derived from Eqs. 2 and 40 given the equilibrium constant κ (derived from a Langmuir isotherm). Surface diffusion constant D_C can be simply derived from R_{SD} by Eq. 40.

Fraction Mobility, Absolute Concentration, and Free Site Fraction

We have thus far assumed a monokinetic reaction process (i.e., a single set of adsorption/desorption and surface diffusion rates). In practice, a multiplicity of k_1, k_2, and D_C constants may be present. In the reaction limit, some form of curve fitting can be reasonably attempted (as in the accompanying paper [26]).

In TIR/FPR, for the special case of a mixture of mobile (reversibly bound and/or surface diffusive) and immobile (irreversibly bound and fixed in place) adsorbed solute, the fraction f of all adsorbed molecules which are mobile can be calculated as in standard FPR (18).

In TIR/FCS for a monokinetic system,

$$\frac{G_c(0)}{\overline{F}^2} = \frac{\beta}{\overline{C}} \frac{\int \mathcal{I}^2(\mathbf{r}) \mathrm{d}^2 r}{\left[\int \mathcal{I}(\mathbf{r}) \mathrm{d}^2 r\right]^2}. \tag{47}$$

We can therefore calculate $\overline{C}$, given experimental values for $G_c(0)/\overline{F}^2$ (from TIR/FCS) and β (from a Langmuir isotherm). More generally, if fraction f of the adsorbed solute is mobile (as determined by TIR/FPR), then in TIR/FCS on the same sample, the right hand side of Eq. 47 should be multiplied by f^2.

Since characteristic times R_R for TIR/FPR and TIR/FCS differ by a factor β, experimental results for R_R taken on the same sample by both variants of the technique can be compared to yield β.

Comparison of TIR/FPR and TIR/FCS

As shown in the preceding sections, TIR/FPR and TIR/FCS yield identical information about the kinetic rate and surface diffusion coefficient, and complimentary information about the mobile fraction, the absolute concentration of mobile adsorbate, and the fraction of sites which are free. Experimentally, the two techniques are also complimentary. TIR/FPR measures the total fluorescence, which increases with a large observation area and a high surface concentration. TIR/FCS measures statistical fluctuations, which increase in relative size with a small observation area and low surface concentration. (High total surface concentration can be used, nevertheless, if the fluorescently-labeled solute is mixed with unlabeled solute.)

Relative to TIR/FCS, TIR/FPR is instrumentally simpler and much less sensitive to spurious sources of noise, but it is more subject to possible photochemically induced artifacts during the bright photobleaching pulse. In TIR/FPR, the profile and the size of the observation region as defined by the focused laser beam is experimentally hard to control. In TIR/FCS, the observation region may be easily defined and controlled by an image plane aperture.

RANGE OF APPLICABILITY

A fundamental requirement of TIR/FPR and TIR/FCS experiments is that measured fluorescence originates primarily from surface adsorbed (rather than bulk solubilized) molecules. As described below, this requirement places an upper bound on the rates of reaction R_R which can be measured by the technique. In addition, the optical resolution of the fluorescence observation system places a lower bound on the surface diffusion coefficients D_C which can be measured.

Upper Bound for Measurable Reaction Rates

The number of bulk molecules per unit area located within an evanescent intensity of characteristic thickness d is $\bar{A}d$. From the equilibrium relation Eq. 2, we can write the ratio of surface adsorbed solute to bulk solute in the field as

$$\bar{C}/\bar{A}d = \kappa(N - \bar{C})/d, \tag{48}$$

where N is the total number of surface sites per unit area. (For a typical TIR experiment involving fluorescent antibodies and surface bound antigen, Kronick [12] found this ratio to be ~50.) For a given κ and $\bar{C}$, one can increase this ratio by increasing N (if the surface is precoated with specific binding site molecules), or by decreasing d. The depth of the evanescent intensity is (14)

$$d = \frac{\lambda_0}{4\pi(n_1^2 \sin^2\phi - n_2^2)^{1/2}}, \tag{49}$$

where λ_0 is the light wavelength in vacuum, n_1 and n_2 are the refractive indices of the denser and less dense media, respectively, and ϕ is the angle of incidence of the light. Thus, d may be decreased by increasing the refractive index of the denser (solid) medium, increasing the angle of incidence, or decreasing the wavelength of the incident light.

The required dominance of surface fluorescence over bulk fluorescence (i.e., $\bar{C}/\bar{A}d \gg 1$), along with Eq. 40, leads to upper bounds for R_{BND} of D_A/d^2 for TIR/FPR and $D_A/(\beta d)^2$ for TIR/FCS.[5] In earlier sections, we have demonstrated that reaction rate R_R cannot be easily extracted from $G(t)$ unless $R_R \lesssim R_{BND}$. Therefore, a reaction rate R_R larger than $\sim D_A/d^2$ cannot be measured. For a strontium titanate-water interface with refractive indecies 2.4 and 1.33, incident light wavelength 476 nm, and incidence angle 85°, (a favorable experimental configuration ensuring a small d), and a protein bulk diffusion coefficient D_A of 5×10^{-7} cm^2/s, the upper bound for R_R is $1.4 \times 10^6\ s^{-1}$.

Whether $G(t)$ is reaction limited or bulk diffusion limited, its decay rate always reflects the actual relaxation rate of the sorption process; the decay rate is not an experimental artifact of the optical system in any limit and it cannot exceed the upper bound for R_{BND} discussed here. If an experimental $G(t)$ has a decay rate which is at or near this upper bound, one may conclude that the process is probably bulk diffusion limited.

Lower Bound for Measurable Surface Diffusion Rates

Unless surface diffusion can laterally transport an adsorbed molecule a distance on the order of the observation size s before it desorbs, surface diffusion will not be detected in the experimental $G(t)$. Thus, surface diffusion can only be detected if $R_{SD} \gtrsim R_R$. For a given coefficient D_C, R_{SD} can be increased by reducing the observation size s. However, s cannot be decreased below the optical resolution of the fluorescence detection system.

DISCUSSION

We have described the theoretical bases of new related methods for obtaining adsorption/desorption reaction rates and surface diffusion coefficients of solute molecules in equilibrium with a solid surface. In this context, "adsorption" can mean either specific binding of soluble ligands to receptors immobilized on the surface, or nonspecific physical (e.g., electrostatic) binding to a surface. Since we assume a finite number of discrete binding sites, "surface diffusion" reflects a preferential hopping from site to site. As the number of sites becomes very large, surface diffusion becomes a smooth lateral motion.

In contrast to other kinetics techniques, such as stopped flow and temperature, pressure and concentration jump, TIR/FPR and TIR/FCS have the following features: (*a*) They are performed with no extrinsic perturbation from chemical equilibrium. (*b*) They require no spectroscopic or thermodynamic change between the dissociated and complexed states of the reaction. (*c*) TIR/FPR can determine the relative amounts of reversible vs. irreversible adsorption and TIR/FCS can determine the absolute concentration of the adsorbate independently of the efficiencies of fluorescence emission and detection. (*d*) As surface chemistry techniques, TIR/FPR and TIR/FCS should be particularly useful where surface adsorption and surface diffusion are important.

TIR/FPR and TIR/FCS may prove useful in the study of many biological systems. There

[5]To achieve larger relative number fluctuations in TIR/FCS experiments, it is necessary either that a large fraction of the surface binding sites be unbound on the average, or, alternatively, that fluorescent-labeled solute is diluted in an excess of unlabeled solute.

is a growing interest in the possible rate enhancement between soluble ligand and specific receptor in a membrane due to nonspecific ligand adsorption followed by surface diffusion (5). TIR/FPR and TIR/FCS are particularly well suited to measuring the surface kinetics parameters relevant to this effect. In addition, important biochemical events are triggered by surface adsorption. An application of TIR/FPR to the study of the adsorption/desorption and surface diffusion of blood proteins on quartz is presented in an accompanying paper (26). TIR/FPR and TIR/FCS can probe molecular dynamics on a surface precoated with molecules that react specifically with the fluorescent-labeled ones in solution. Thus, the technique can be used to study immobilized antigen-antibody reactions, immobilized hormone receptor-hormone reactions, and immobilized enzyme-substrate reactions.

APPENDIX

Calculation of G(t) by Computer

We define $\alpha \equiv \nu + (R_{BLD}/R_R)\xi^2$, and note that (28):

$$L^{-1}_{\nu \to R_R t} N(\xi, \nu) = e^{R_{BLD}\xi^2 t} L^{-1}_{\alpha \to R_R t} N(\xi, \alpha - \xi^2 R_{BLD}/R_R). \tag{A1}$$

Using Eq. A1 and replacing ν with $\alpha - \xi^2 R_{BLD}/R_R$ in Eq. 39 yields

$$L^{-1}_{\nu \to R_R t} N(\xi, \nu) = e^{R_{BLD}\xi^2 t} L^{-1}_{\alpha \to R_R t} \cdot \left\{ \frac{\sqrt{\alpha} + \sqrt{\dfrac{R_R}{R_{BND}}}}{\alpha^{3/2} + \sqrt{\dfrac{R_R}{R_{BND}}}\,\alpha + \left(1 + \dfrac{R_{SD} - R_{BLD}}{R_R}\xi^2\right)\bar{\alpha} + \dfrac{R_{SD} - R_{BLD}}{R_R}\sqrt{\dfrac{R_R}{R_{BND}}}\,\xi^2} \right\}. \tag{A2}$$

After rewriting Eq. A2 as six partial fractions, inverse Laplace transforming (28) and using Eq. A2 in Eq. 38, we find that

$$\frac{G(t)}{G(0)} = \frac{\int |\mathcal{I}'(\xi)|^2 e^{-R_{BLD}\xi^2 t} \sum_{i=1}^{3} \dfrac{\alpha_i^{1/2}\left(\alpha_i^{1/2} + \sqrt{\dfrac{R_R}{R_{BND}}}\right)}{(\alpha_i^{1/2} - \alpha_j^{1/2})(\alpha_i^{1/2} - \alpha_k^{1/2})} w[-i(\alpha_i R_R t)^{1/2}] d^2\xi}{\int |\mathcal{I}'(\xi)|^2 d^2\xi}, \tag{A3}$$

where $\alpha_1^{1/2}$, $\alpha_2^{1/2}$, and $\alpha_3^{1/2}$ are the three roots of the denominator of Eq. A2, and are functions of the four characteristic rates and ξ^2. In the sum over i, $\alpha_j^{1/2}$ and $\alpha_k^{1/2}$ are the two roots other than $\alpha_i^{1/2}$ for each i. Eq. A3 is an exact form of $G(t)$ for any values of R_R, R_{BND}, R_{BLD}, R_{SD}, and t. The integral may be calculated using a numerical integration technique; w-functions may be approximated by infinite series for small or large arguments (28) or calculated directly from Eq. 43.

We thank Ms. Shirley Mieras and Ms. Mae Gillespie for typing the manuscript. This work was supported by the following grants: Research Corporation Cottrell Research Grant; American Chemical Society-Petroleum Research Fund grant 10590-G5,6; University of Michigan Rackham Faculty Research Grant; and National Institutes of Health grants 1R01-NS14565 and 1R01-HL24039.

Received for publication 10 June 1980.

REFERENCES

1. MOSBACH, K., EDITOR. 1976. Immobilized Enzymes. *Methods Enzymol.* Vol. 64.
2. LARTIQUE, D. J., and S. YAVERBAUM. 1976. Enzymes immobilized on glass. *In* Progress in Surface and Membrane Science. D. A. Cadenhead, and J. F. Danielli, editors. Academic Press, Inc., New York. 361.
3. IVAR, G. 1978. A simple visual surface immunology test. *J. Immunol. Methods.* **24**:57.
4. WEETAL, H. H. 1972. Insolubilized antigens and antibodies. *In* The Chemistry of Biosurfaces. M. L. Hair, editor. Marcel Dekker, Inc., New York. 597.
5. ADAM, G., and M. DELBRÜCK. 1968. Reduction of dimensionality in biological diffusion processes. *In* Structural Chemistry and Molecular Biology. A. Rich, and N. Davidson, editors. Freeman, San Francisco.
6. ROBERTS, H., and B. HESS. 1977. Kinetics of cytochrome *c* oxidase from yeast: membrane-ficilitate electrostatic binding of cytochrome *c* showing a specific interaction with cytochrome *c* oxidase inhibition by ATP. *Biochim. Biophys. Acta.* **462**:215.
7. WONG, M., M. E. BAYER, and S. LITWIN. 1978. Virus-cell interaction: prediction of the time course of observable effects from virus interaction at cell injection sites, and mechanisms leading to attachment. *FEBS Lett.* **95**:26.
8. EIGEN, M. 1974. Diffusion control in biochemical reactions. *In* Quantum Statistical Mechanics in the Natural Sciences. B. Kursunoglu, S. L. Mintz, and S. M. Widmayer, editors. Plenum Press, New York. 37.
9. BERG, 0. G., and C. BLOMBERG. 1976. Association kinetics with coupled diffusional flows. Special application to the lac repressor-operator system. *Biophys. Chem.* **4**:367.
10. WEAVER, D. L. 1979. Diffusional-controlled mean reaction times in biological systems with elliptical symmetry. *Biophys. Chem.* **10**:245.
11. SCHRANNER, R., and P. H. RICHTER. 1978. Rate enhancement by guided diffusion: chain length dependence of repressor-operator association rates. *Biophys. Chem.* **8**:135.
12. KRONICK, M. 1974. Sensing of structure-specific binding onto functionalized quartz surfaces using total internal reflection fluorescence. Ph.D. Thesis. Stanford University, Stanford, Calif.
13. WATKINS, R. W., and C. R. ROBERTSON. 1977. A total internal reflection technique for the examination of protein adsorption. *J. Biomed. Mater. Res.* **11**:915.
14. HARRICK, N. J. 1967. Internal Reflection Spectroscopy. John Wiley & Sons Inc., New York.
15. HIRSCHFELD, T. 1965. Total reflection fluorescence (TRF). *Canadian Spectroscopy.* **10**:128.
16. HIRSCHFELD, T., and M. J. BLOCK. 1977. Virometer: realtime virus detection and identification in biological fluids. *Opt. Eng.* **16**:406.
17. HARRICK, N. J., and G. I. LOEB. 1973. Multiple reflection fluorescence spectrometry. *Anal. Chem.* **45**:687.
18. AXELROD, D., D. E. KOPPEL, J. D. SCHLESSINGER, E. L. ELSON, and W. W. WEBB. 1976. Mobility measurement by analysis of fluorescence photobleaching recovery kinetics. *Biophys. J.* **16**:1055.
19. CHERRY, R. J. 1979. Rotational and lateral diffusion of membrane proteins. *Biochim. Biophys. Acta.* **559**:289.
20. ELSON, E. L., and D. MAGDE. 1974. Fluorescence correlation spectroscopy. I. Conceptual basis and theory. *Biopolymers.* **13**:1.
21. MAGDE, D., E. L. ELSON, and W. W. WEBB. 1974. Fluorescence correlation spectroscopy. II. An experimental relization. *Biopolymers.* **13**:29.
22. KOPPEL, D. E. 1974. Statistical accuracy in fluorescence correlation spectroscopy. *Phys. Rev. A.* **10**:1938.
23. RIGLER, R., P. GRASSELLI, and M. EHRENBERG. 1979. Fluorescence correlation spectroscopy and application to the study of Brownian motion of biopolymers. *Physica. Scripta.* **19**:486.
24. ARAGON, S. R., and R. PECORA. 1976. Fluorescence correlation spectroscopy as a probe of molecular dynamics. *J. Chem. Phys.* **64**:1791.
25. BOREJDO, J., S. PUTNAM, and M. F. MORALES. 1979. Fluctuations in polarized fluorescence: evidence that muscle cross bridges rotate repetitively during contraction. *Proc. Natl. Acad. Sci. U.S.A.* **76**:6346.
26. BURGHARDT, T. P., and D. AXELROD. 1981. Total internal reflection/fluorescence photobleaching recovery study of serum albumin adsorption dynamics. *Biophys. J.* **33**:455–467.
27. FEHER, G., and M. WEISSMAN. 1973. Fluctuation spectroscopy: determination of chemical reaction kinetics from the frequency spectrum of fluctuations. *Proc. Natl. Acad. Sci. U.S.A.* **70**:870.
28. ABRAMOWITZ, M., and I. STEGUN, EDITORS. 1972. Handbook of Mathematical Functions. National Bureau of Standards, Washington, D.C.